Numerical analysis of the Temperature Distribution in Centrifugal Casting

J. A. AKPOBI*, I. D. ERHUNMWUN** and T. A. OSUNDE***

* Department of Production Engineering, University of Benin, Benin City, Nigeria

**Department of Production Engineering, University of Benin, Benin City, Nigeria, +2348070728898

** Nigeria Prisons Staff School, behind medium security prisons, Oko, GRA, Benin City,Nigeria +2348060464049

(john.akpobi@uniben.edu; Mobile+2348055040348)

Received: 08.11.2018 Accepted:13.03.2019

Abstract- This paper entails the mathematical modelling of the conductive heat transfer in horizontal centrifugal casting. The model was then used to analyse the temperature distribution in centrifugal casting. The Finite Element Method was used to discretize and analyse the temperature distribution. Four quadratic element was used to represent the entire domain of the casting and mould region respectively. The result obtained shows the temperature distribution both in the liquid cast region and the mould region. The liquid cast was poured into the prepared mould at the temperature of 15000C and the mould was preheated to a temperature of 2500C to prevent thermal shock. After about 20 secs when the liquid cast has been poured into the mould, the result obtained shows a decrease in temperature from 1388.72950C at a distance of 4.5cm to 1032.86360C at a distance of 6.5cm from the centre of the mould. Also in the mould region, after about 20 secs, the temperature drops from 755.82520C at 6.5cm to 350.62050C at 15.5cm from the centre of the mould. The maximum percentage error was 1.6627% and the minimum percentage error was 0.0069%. This comparison was made for the temperature distribution in the cast region and the mold region after about 20 secs when the molten metal has been poured into the mold cavity. This shows that the result obtained from this research is in agreement with the result obtained from finite difference method.

Keywords- Centrifugal Casting, Finite Element Method, Heat Transfer, Discretization, Conduction.

1. Introduction

"Metal casting is a shape forming process whereby molten metal is poured into a prepared mould and allowed to solidify such that the shape of the solidified object is determined by the shape of the mould cavity" [1]. The solidified part is also known as a casting, which is ejected or broken out of the mould to complete the process. The products made by centrifugal casting have better integrity than the components made by permanent mould Casting Process [2]. Casting materials are usually metals or various cold setting materials that cure after mixing two or more components together; examples are: concrete, clay and plaster [3]. The solidification of materials depends on the cooling rate of the materials which is governed by heat flow in the mould and alloy composition [4]. Solidification rate also affects the structure and properties of the materials. Solidification takes place through nucleation and growth of the solid phase under favourable thermal conditions.

The technological difficulties involved in casting processes vary considerably according to the metal's melting temperature characteristics, which in turn are related to the physicochemical properties and structures of metals and alloys. These difficulties also involve a series of properties, which include differences in chemical activities between the elements that constitute the alloy, solubility of the gases, method of solidification among the chemical elements, type of molding, and coefficients of solidification shrinkage. On the other hand, the cooling process also affects the flow of cast metal, influencing the mold filling and stability, allowing the occurrence of cooling stresses and properties changes in the final product, and producing variations in the geometrical dimensions, the shape of the surface finish and the quality of the cast part. Some of the properties and characteristics most directly associated with the casting process are as follows, given by [5].

In 2001, a study was carried out by Kamlesh, by using the finite difference method to determine the temperature distribution in horizontal centrifugal casting. This was done

both in the liquid cast and mould region [6]. A study was also carried out by Anjo in 2012 to numerically stimulate the steady conduction heat transfer during the solidification of aluminum in green sand mould using finite difference analysis in 2D [7]. The numerical simulation of the process of centrifugal casting is challenging, the description of its numerical simulation is not replete in literature. Some papers describe the less complex vertical centrifugal casting process [8].

Therefore, this research paper sort to look into the temperature distribution in horizontal centrifugal casting under the condition that none of the liquid cast solidifies the moment it's been poured into the mould. This research also covers both the temperature distribution in the liquid cast region and the mould region.

2. E-signature Methods

The mathematical models used in centrifugal casting are based especially on heat transfer and solidification consideration of centrifugal casting. A schematic representation of the model of the centrifugal casting is shown in Fig. 1. The heat is withdrawn from the liquid region of the casting to the metallic mould, and finally from mould to surrounding. Heat is also radiated away from the inner surface of the casting. As the solidification proceeds by conductive heat transfer through the molten metal in contact with metallic mould, the solid-liquid interface moves away from the metallic mould.

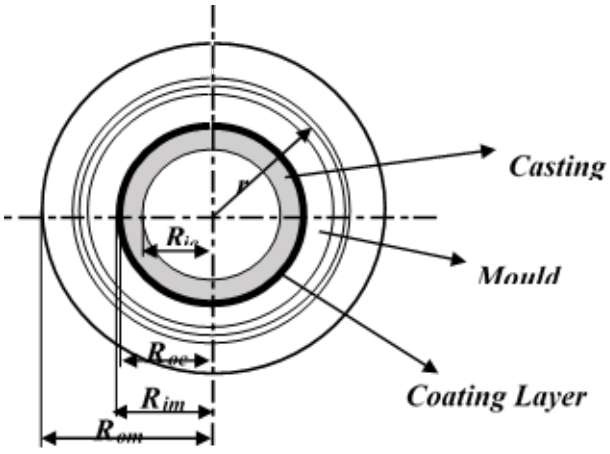

Fig. 1. Geometry of horizontal-axis centrifugal casting

The transient radially symmetric heat flow in the cylinder is governed by:

$$\frac{1}{r}\frac{\partial}{\partial r}\left(k_\xi r\frac{\partial T_\xi}{\partial r}\right)=C_\xi\rho_\xi\frac{\partial T_\xi}{\partial t} \qquad 1$$

Before pouring the melt into the mould, the mould is preheated to a certain temperature to avoid thermal damage to the mould. Therefore, the initial temperature distributions in the casting, mould and shell regions are taken as:

$$T_c = T_p \qquad 2$$

$$T_g = T_m = T_M \qquad 3$$

As soon as the melt comes in contact with the mould wall, temperature of the metal-mould interface increases suddenly. Initial interface temperature is approximated by considering thermal energy conservation within the very thin layer of the metal and the mould in an adiabatic system (Ebisu, 1977; Phelke et al., 1978). Since the heat flow rate from the metal to mould at the beginning is very rapid indeed, it can be stated that the liquid metal within this layer solidifies instantaneously.
In order to find the metal-coating layer interface temperature at time t=0, the mould is assumed to be at a temperature TM and the initial temperature of casting is assumed to be the temperature of the metal as it enters the mould cavity. To find a reasonable approximation to the initial interface temperature, consider an adiabatic system shown in Fig. 2.

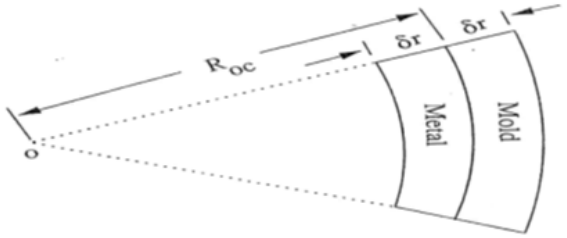

Fig. 2: Control volume considered when calculating the initial temperature of metal-mould interface [9]

Equating the thermal energy in the system initially to that in the system at equilibrium yields

$$2\pi R_{oc}\partial r\left(\rho_g C_g T_M+\rho_L C_L T_p\right)=2\pi R_{oc}\partial r\left(\rho_g C_g+\rho_L C_L\right)T_0 \qquad 4$$

where T_0 is the initial metal-coating layer interface temperature. On rearranging the terms the interface temperature can be written as:

The boundary conditions in different regions of the casting and mould are as follows:

$$T_0=\frac{\rho_g C_g T_M+\rho_L C_L T_p}{\rho_g C_g+\rho_L C_L} \qquad 5$$

1. At the inner surface of the casting, i.e., at $r = R_{ic}$

$$k_{lc}\frac{\partial T_{lc}}{\partial r}=h_2\left(T_{ci}-T_\beta\right) \qquad 6$$

Where $T_\beta = \frac{T_p + T_a}{2}$ 7

In the development of the weak form, we assumed a linear mesh and placed it over the domain. This was done by multiplying Eq. 1 by the weighted function (w) and integrating the final Equation over the domain. This results in the mathematical expression in Eq. 8.

$$\frac{k_\xi}{C_\xi \rho_\xi}\int_{r_A}^{r_B} r\frac{\partial w}{\partial r}\frac{\partial T_\xi}{\partial r}dr + \int_{r_A}^{r_B} w\frac{\partial T_\xi}{\partial t}rdr - wQ_A - wQ_B = 0 \quad 8$$

Where

$$-Q_A = \frac{wk_\xi r}{C_\xi \rho_\xi}\frac{\partial T_\xi}{\partial r}\bigg|_{r_A} \text{ and } Q_B = \frac{wk_\xi r}{C_\xi \rho_\xi}\frac{\partial T_\xi}{\partial r}\bigg|_{r_B} \quad 9$$

Eq. 8 is referred to as the weak form of the governing

In the weak form, since the primary variable is simply the function itself, the Lagrange family of interpolation functions is admissible, therefore:

$$T_\xi(r,t) = \sum_{j=1}^{n}\left(T_\xi\right)_j(t)\psi_j^e(r) \quad and \quad w = \psi_i^e(r) \quad 10$$

Substituting eq. 10 into eq. 8, we have:

$$\left[K_{ij}^e\right]\left\{T_\xi\right\}_j + \left[M_{ij}^e\right]\left\{\dot{T}_\xi\right\}_j = \left\{Q_i^e\right\} \quad 11$$

Where $$K_{ij}^e = \frac{k_\xi}{C_\xi \rho_\xi}\int_{r_A}^{r_B} r\frac{\partial \psi_i^e}{\partial r}\frac{\partial \psi_j^e}{\partial r}dr$$ (Conductivity Matrix) 12

$$M_{ij}^e = \int_{r_A}^{r_B} r\psi_i^e\psi_j^e dr \quad \text{(Enthalpy Matrix)} \quad 13$$

Next, we use the already developed finite element model of one-dimensional time-dependent problem to describe time approximation schemes and also convert the ordinary differential equation in time to algebraic equation. The most commonly used method for solving eq. 11 is the family of interpolation in which a weighted average of the time derivative of the dependent variable is approximated to two consecutive time steps by linear interpolation of the values of the variables of the two steps. Therefore, we have:

$$\left[\left[M_{ij}^e\right] + \Delta t_{s+1}\alpha\left[K_{ij}^e\right]\right]\left\{T_\xi\right\}_{j_{s+1}} = \left[\left[M_{ij}^e\right] - \Delta t_{s+1}(1-\alpha)\left[K_{ij}^e\right]\right]\left\{T_\xi\right\}_{j_s} + \Delta t_{s+1}(1-\alpha)\left\{Q_i^e\right\}_s + \Delta t_{s+1}\alpha\left\{Q_i^e\right\}_{s+1}$$

14

Using the Backward Difference Scheme, where , eq. 14 is reduced to eq. 15

The assembled K^e matrix is given as:

2.1. Evaluating the elemental matrices

The one-dimensional Lagrange quadratic interpolation function for the equation becomes:

$$\psi_1(r) = \frac{1}{h_e^2}(h_e + r_A - r)(h_e - 2r + 2r_A) \quad 16$$

$$\psi_2(r) = \frac{4}{h_e^2}(r - r_A)(h_e + r_A - r) \quad 17$$

$$\psi_3(r) = \frac{-1}{h_e^2}(r - r_A)(h_e - 2r + 2r_A) \quad 18$$

The Conductivity matrix can be easily derived by substituting the Lagrange interpolation functions in eq. 16 to 18 into eq. 12 respectively, we have:

$$\left[K^e\right] = \frac{k_\xi}{6h_eC_\xi\rho_\xi}\begin{bmatrix} 3h_e+14r_A & -(4h_e+16r_A) & h_e+2r_A \\ -(4h_e+16r_A) & 16h_e+32r_A & -(12h_e+16r_A) \\ h_e+2r_A & -(12h_e+16r_A) & 11h_e+14r_A \end{bmatrix} \quad 19$$

Also, the Enthalpy matrices can be easily derived by substituting the Lagrange interpolation functions in eq. 16 to 18 into eq. 13 accordingly, we have:

$$\left[M^e\right] = \frac{h_e}{60}\begin{bmatrix} h_e+8r_A & 4r_A & -h_e-2r_A \\ 4r_A & 16h_e+32r_A & 4h_e+4r_A \\ -h_e-2r_A & 4h_e+4r_A & 7h_e+8r_A \end{bmatrix} \quad 20$$

$$K^e = \frac{k_\xi}{6hC_\xi\rho_\xi}\begin{bmatrix} 3h_e+14r_w & -(4h_e+16r_w) & h_e+2r_w & 0 & 0 & 0 & 0 & 0 & 0 \\ -(4h_e+16r_w) & 16h_e+32r_w & -(12h_e+16r_w) & 0 & 0 & 0 & 0 & 0 & 0 \\ h_e+2r_w & -(12h_e+16r_w) & 28h_e+28r_w & -(20h_e+16r_w) & 3h_e+2r_w & 0 & 0 & 0 & 0 \\ 0 & 0 & -(20h_e+16r_w) & 48h_e+32r_w & -(28h_e+16r_w) & 0 & 0 & 0 & 0 \\ 0 & 0 & 3h_e+2r_w & -(28h_e+16r_w) & 56h_e+28r_w & -(36h_e+16r_w) & 5h_e+2r_w & 0 & 0 \\ 0 & 0 & 0 & 0 & -(36h_e+16r_w) & 80h_e+32r_w & -(44h_e+16r_w) & 0 & 0 \\ 0 & 0 & 0 & 0 & 5h_e+2r_w & -(44h_e+16r_w) & 84h_e+28r_w & -(52h_e+16r_w) & 7h_e+2r_w \\ 0 & 0 & 0 & 0 & 0 & 0 & -(52h_e+16r_w) & 112h_e+32r_w & -(60h_e+16r_w) \\ 0 & 0 & 0 & 0 & 0 & 0 & 7h_e+2r_w & -(60h_e+16r_w) & 53h_e+14r_w \end{bmatrix} \quad 21$$

The assembled M^e matrix is given as:

$$M^e = \frac{h_e}{60}\begin{bmatrix} h_e+8r_w & 4r_w & -h_e-2r_w & 0 & 0 & 0 & 0 & 0 & 0 \\ 4r_w & 16h_e+32r_w & 4h_e+4r_w & 0 & 0 & 0 & 0 & 0 & 0 \\ -h_e-2r_w & 4h_e+4r_w & 16h_e+16r_w & 4h_e+4r_w & -3h_e-2r_w & 0 & 0 & 0 & 0 \\ 0 & 0 & 4h_e+4r_w & 48h_e+32r_w & 8h_e+4r_w & 0 & 0 & 0 & 0 \\ 0 & 0 & -3h_e-2r_w & 8h_e+4r_w & 32h_e+16r_w & 8h_e+4r_w & -5h_e-2r_w & 0 & 0 \\ 0 & 0 & 0 & 0 & 8h_e+4r_w & 80h_e+32r_w & 12h_e+4r_w & 0 & 0 \\ 0 & 0 & 0 & 0 & -5h_e-2r_w & 12h_e+4r_w & 48h_e+16r_w & 12h_e+4r_w & -7h_e-2r_w \\ 0 & 0 & 0 & 0 & 0 & 0 & 12h_e+4r_w & 112h_e+32r_w & 16h_e+4r_w \\ 0 & 0 & 0 & 0 & 0 & 0 & -7h_e-2r_w & 16h_e+4r_w & 31h_e+8r_w \end{bmatrix} \quad 22$$

$$\{Q^e\} = \begin{Bmatrix} Q_1^1 \\ 0 \\ 0 \\ 0 \\ 0 \\ 0 \\ 0 \\ 0 \\ Q_3^4 \end{Bmatrix} \quad 23$$

3. Result and Discussion

The model has been implemented by using following thermo physical properties (for casting and mould material), and design and operating parameters. 25% Cr-20% Ni steel is chosen as molten metal and 0.4% Carbon steel as mould material to validate the developed model with results available in literature. Various design and operating parameters, like geometric constants for the casting and the mould, the heat transfer coefficient at different regions of casting and the mould, and initial temperatures of mould and metal used in the analysis are tabulated in Table 1.

K_d ($cal/cmsec^0C$) at 0^0C	0.025	0.126	$2x10^{-2}$
$\rho(gr/cm^3)$	7.3	7.8	5.7
$C(cal/gm^0C)$	0.118	0.1	0.08
$T_s(^0C)$	1300	-	-
$T_L(^0C)$	1400	-	-
$T_f(^0C)$	1300	-	-
$\Delta H(cal/gr)$	60	-	-

Table 1: Thermo physical properties of casting, mould material, and coating layer

Thermo Physical Properties	25%Cr-20%Ni Steel	0.4% Carbon Steel	Coating Layer

Outer diameter of steel mould, (cm)	31
Outer diameter of casting, (cm)	13

Inner diameter of casting, (cm)	9
Damping coefficient between the mould-metal interface, β	0.83
Heat transfer coefficient at outer surface of steel mould (h_2) and at inner surface of casting (h_1), (cal/cm^2sec^0C)	0.0002
Initial pouring temperature, $T_p(^0C)$	1500
Initial mould temperature, $T_m(^0C)$	250
Ambient temperature, $T_a(^0C)$	25
Emissivity at outer surface of mould, $\mathcal{E}_M$	0.4

Table 2: Design and operating parameters used in analysis

In this analysis, the initial temperature of the liquid cast at time t=0 as shown in Table 2 was taken to be 15000C. This temperature represents the temperature of the liquid cast as it is been poured into the mould known as the Pouring Temperature. Also, to prevent the mould from collapsing due to a sudden change in temperature, the mould was preheated to a temperature of 2500C. This temperature represents the initial Mould Temperature. Before pouring the liquid cast into the mould, the temperature of the air in the mould and outside the mould was taken to be 250C. This represents the Ambient Temperature.

In this case, as the liquid metal is poured into the mould, it is assumed that none of the liquid metal cast solidifies. As the liquid metal is been poured into the mould at the liquid metal/mould interface, the temperature of the liquid metal drops significantly and that of the mould increases significantly. The system is therefore assumed to be allowed to come to equilibrium adiabatically. The adiabatic assumption is reasonable because as whatever happens to the system, it is assumed to happen instantly. Also, by definition of this condition, no heat flux has yet been established, hence no heat is transferred to or from the system. This sudden change in the temperature of the liquid metal cast and mould interface can be estimated using eq. 5.

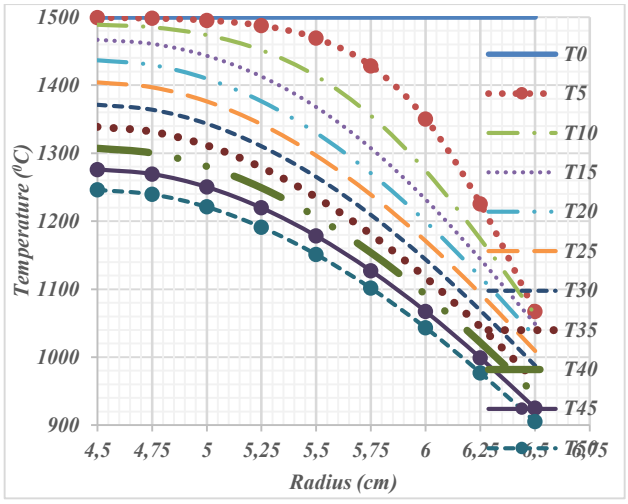

Fig. 3: A graph of Temperature against Radius in the liquid metal region

Fig. 3 shows a graph of temperature against the radial displacement at different time within the liquid metal cast region. From the graph, it is observed that the region between 0cm and 4.5cm is not presented. This region is hollow and the temperature in this region is determined by taking the temperature average between the pouring temperature and the ambient temperature. This is shown in eq. 7.

From Fig. 3, it is observed that there is a decrease in temperature in the liquid metal cast. This is due the fact that the heat in the system is conducted away from the liquid cast. This decrease in temperature was very pronounced in the region close to the liquid cast / mould interface. The reason for this sudden change in temperature is that as the liquid cast is poured into the mould, the mould quickly conducts the heat away from the liquid cast / mould interface. Also, at the interface between the hollow cast, there is also a decline in temperature as time increases. This is because the heat in the liquid cast is released into the atmosphere.

Fig. 4 shows a graph of temperature against the radial displacement at different time within the mould region. From the graph, it is observed that the region between 6.5cm and 15.5cm is not presented. This region contains the liquid metal cast and the temperature in this region is as presented in Fig. 3.

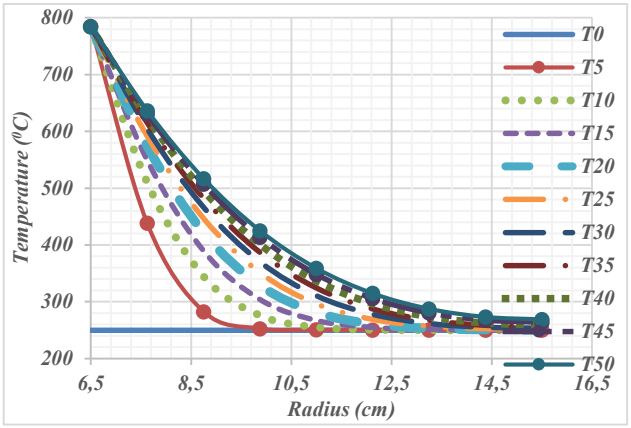

Fig. 4: A graph of Temperature against Radius in the mould region

From Fig. 4, it can be seen that the mould is preheated to a temperature of 2500C. As the liquid cast is poured into the mould, it is observed that there is a sudden increase in temperature at the liquid metal cast / mould interface. This is due the fact that the heat in the liquid cast is conducted away from the liquid cast into the mould. This increase in temperature was very pronounced in the region close to the liquid cast / mould interface. This sudden temperature increase at the interface decreases towards the outer surface of the mould. As time increases, there is a decline in temperature and the heat in the system is finally released into the atmosphere.

Fig. 5 shows a graph of temperature against radial displacement at different time. Between 4.5cm and 6.5cm is the liquid cast region and between 6.5cm and 15.5cm is the mould region. Along the 6.5cm line in the radial axis is the interface between the liquid cast region and the mould region. Along the interface, there is a sudden drop in temperature.

Fig. 5 shows a graph of temperature against radius for the mould region and liquid cast region. As the liquid metal is

poured into the mould, the temperature at the inlet begins to decrease. At about 10sec after pouring the molten metal into the mould, the temperature at the inner surface of the liquid matal cast would have droped to about 1489.07270C and at about 50sec after pouring, the temperarure would have droped to about 1246.09770C. Still at 50sec after pouring and at the liquid metal cast / mould interface, the temperature droped suddenly from 905.18520C at the liquid metal cast region to 784.42210C at the mould region. There after in the mould region, the temperature begins to drop steadily till the outer surface of the mould where the temperature is lost to the atmosphere.

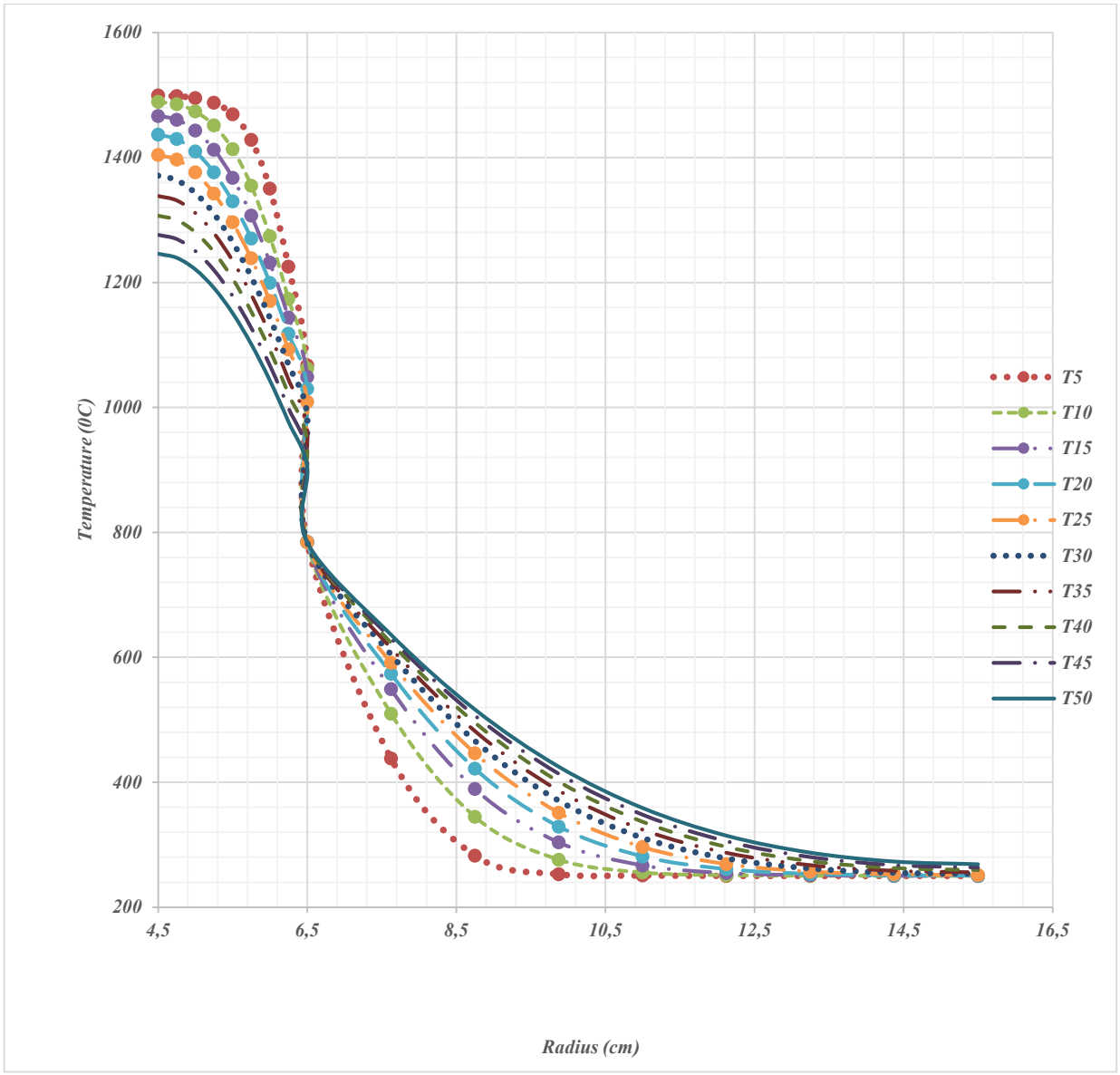

Fig. 5: A graph of Temperature against Radius in the liquid cast and mould region

3.1. Comparison with Results Available in Literature

The temperature profiles obtained by this research, for different operating conditions have been shown above in Fig. 3 to Fig. 5. It is clear that the trend of temperature profiles obtained this research using the Finite Element Method is similar to those obtained by Kamlesh (2001) with some percent of error. It is evident form the graphs for temperature profiles that solidification starts from the molten metal in contact with the inner mold wall and proceeds right across the inner section until last solidifying metal freezes at inner bore, therefore the chances of shrinkage cavity is more at inner bore as compare to other region of solidifying metal.

To validate the result from this research, we compare our result with the result obtained by Kamlesh (2001) where the author used the Finite Difference Method with some disadvantages. Table 3 shows the percentage error between the result from this research and the result obtained by Kamlesh (2001). From the table, the maximum percentage

error was 1.6627% and the minimum percentage error was 0.0069%. This comparison was made for the temperature distribution in the cast region and the mold region after about 20 secs when the molten metal has been poured into the mold cavity. This shows that the result obtained from this research is in agreement with the result obtained from Kamlesh (2001).

	TEMPERATURE (^{0}C)		
RADIUS (cm)	THIS WORK (FEM)	RESULT FROM KAMLESH (2001)	PERCENTAGE ERROR (%)
4.5000	1388.7295	1380	-0.6326
4.7500	1382.4987	1380	-0.1811
5	1364.5767	1363	-0.1157
5.2500	1335.0924	1335	-0.0069
5.5000	1294.1723	1300	0.4483
5.7500	1242.2417	1245	0.2216
6	1180.3040	1180	-0.0258
6.2500	1109.4805	1100	-0.8619
6.5000	1032.8636	1035	0.2064
6.5000	755.8252	760	0.5888
7.6250	623.8714	625	0.1806
8.7500	498.1473	490	-1.6627
9.8750	420.0595	420	-0.0142
11	378.7006	378	-0.1853
12.1250	360.3898	360	-0.1083
13.2500	353.3674	353	-0.1041
14.3750	351.0809	351	-0.0230
15.5000	350.6205	350	-0.1773

Table 3: Percentage error between result from this work and Kamlesh (2001)

4. Conclusion

In this study, the finite element method has been used to obtain the temperature distribution in horizontal centrifugal casting. The results obtained from the FEM were compared with the results obtained from the finite difference method and it was discovered that both results agrees. The result obtained shows that the finite element method is an efficient and accurate method.

References

[1] Ibhadode, A. O. A. Introduction to Manufacturing Technology, TETFUND Edition, Ambik publishers, Benin City, Nigeria, 2014.

[2] Shaliesh, P., Praveen Kumar, B., Vijaya Kumar, K. and Nagendra, A. Determination of the Solidification Time of Al-7%Si Alloy during Centrifugal Casting. International Journal of Current Engineering and Technology, vol. 2, pp. 226-229, 2014. DOI: http://dx.doi.org/10.14741/ijcet/spl.2.2014.40

[3] Degarmo, E.P., Black, J.T. and Kohser R.A, Materials and Processes in Manufacturing, 9th Edition, Wiley Inc, USA, 2003.

[4] Shaha, S.K., Haque, M.M., Simulation of Heat Flow in Computational Method and Its Verification on the Structure and Property of Gray Cast Iron, American Journal of Applied Sciences, 7(6), p. 795-799, 2010.

[5] Campbell, J. "Casting", Butterworth-Heinemann, Oxford, 1991.

[6] Kamlesh (2001): Ph.D. Thesis, BVM Engineering College, Gujarat, India, p. 35.

[7] Anjo, V. Numerical Simulation of Steady State Conduction Heat Transfer during the Solidification of Aluminum Casting in Green Sand Mould. Leonardo Electronic Journal of Practices and Technologies, vol. 20, pp. 15-24, 2012.

[8] Kaschnitz, Z. Numerical simulation of centrifugal casting of pipes IOP Conf. Series: Materials Science and Engineering 33012031, 2012.

[9] Raju, P.S.S. and Mehrotra, S.P., (2000). Mater. Trans. JIM, vol. 41, pp. 1626–1635.